Distributed Target Detection using Quantized Measurements for Cooperative MIMO Radar and Communications

Zhen Wang[‡#] and Qian He[#‡*]

[‡]University of Electronic Science and Technology of China, Chengdu, Sichuan 611731, China
[#]Yangtze Delta Region Institute Quzhou, University of Electronic Science and Technology of China, Quzhou, Zhejiang 324000, China

***Abstract*—Distributed target detection is studied for the emerging integrated radar and communications (IRC) systems, where the radar and communications work cooperatively. To cope with the significant hardware complexity, we consider the use of low resolution analog-to-digital converters (ADC). The distributed radar receivers transfer their local received signals to a fusion center (FC) after quantization for a final decision making. For the cooperative IRC system, the detection probability for the likelihood ratio test is derived and the impact of quantization on performance is investigated. Futher, we compare the cooperative IRC system with its non-cooperative counterpart, demonstrating that the cooperation between the radar and communications systems can help improve the radar detection performance.**

***Index Terms*—Integrated radar and communications, distributed target detection, cooperation, quantization.**

I. Introduction

Radar and communications systems have been developing in parallel for decades. However, many developing applications, such as automotive systems [1], [2] or 6G communications networks [3], [4], require simultaneous communications and sensing of the environment, resulting in an unavoidable tendency toward the development of integrated radar and communications (IRC) systems [5]–[8].

In these prospective IRC applications, low-complexity local sensors are often employed, which are equipped with low resolution analog-to-digital converters (ADC) to reduce the hardware costs and power consumption [9]. Therefore, in an IRC system, it is vital to investigate the impact of quantization on performance in an IRC system. In [10]–[12], the radar target parameter estimation has been studied for an IRC system employing 1-bit quantization. Based on the low-precision quantization, [13] discussed the communications signal detection for an IRC system, and [14] designed the optimal precoder for a multi-antenna IRC system by minimizing the radar beampattern error. In [15], the communications receivers in the dual-function IRC system are designed to extract the communications information from the quantized samples. In the existing studies on quantization for the IRC system, there is limited work on radar detection employing quantized measurements. In this study, we discuss the target detection problem for the IRC system using quantized measurements.

Although most of the investigations on IRC systems treat radar and communications signals as interfering with one another, appropriate cooperation may result in improved performance for the integrated system, where, for example, the radar performance can be made beyond the constraints of the traditional radar [16]–[18]. This paper concentrates on the problem of target detection in a cooperative IRC system with distributed radar and communications stations, where the cooperation of the two systems implies the information sharing [16]. The received signals are quantized at each local sensor and sent to the FC. Based on the quantized measurements, the optimal likelihood ratio detector for target detection is obtained at the FC, and the detection performance is derived. The performance of the cooperative system is compared with that of the non-cooperative system.

II. Signal Model

Consider a distributed cooperative IRC system with M_R radar transmitters, N radar receivers, and M_C communications transmitters. The signals emitted by the mth ($m = 1, ..., M_R$) radar transmitter and the m'th ($m' = 1, ..., M_C$) communications transmitter are $\sqrt{E_{R,m}}s_{R,m}(kT_s)$ and $\sqrt{E_{C,m'}}s_{C,m'}(kT_s)$ respectively, where $E_{R,m}$ and $E_{C,m'}$ denote the transmit power, T_s is the sampling period, and $k\,(k = 1, ..., K)$ is an index running over the different time samples. The target, if present, is located at (x, y) moving with velocity (v_x, v_y). The signal received at radar receiver n at time kT_s can be modeled as [16]

$$\begin{aligned} r_n[k] = &\sum_{m=1}^{M_R} \sqrt{E_{R,m}}\zeta_{R,nm}s_{R,m}(kT_s - \tau_{R,nm})e^{j2\pi f_{R,nm}kT_s} \\ &+ \sum_{m'=1}^{M_C} \sqrt{E_{C,m'}}\zeta_{C,nm'}s_{C,m'}(kT_s - \tau_{C,nm'})e^{j2\pi f_{C,nm'}kT_s} \\ &+ w_n[k], \end{aligned} \tag{1}$$

in which the first and second terms are from the radar and communications transmissions respectively. The $\tau_{R,nm}$ and $\tau_{C,nm'}$ represent the corresponding time delays, $\zeta_{R,nm}$ and $\zeta_{C,nm'}$

*Correspondence: qianhe@uestc.edu.cn

This work was supported by the Municipal Government of Quzhou under Grant Number 2021D005.

stand for the corresponding target reflection coefficients (assumed known possibly via preprocessing), and $f_{R,nm}$ and $f_{C,nm'}$ denoete the corresponding Doppler frequencies. The clutter-plus-noise $w_n[k]$ is assumed zero-mean white complex Gaussian distributed with $\mathbb{E}\{w_n[k]w_n^*[k']\} = \sigma_w^2\delta[k-k']$ and $\mathbb{E}[\cdot]$ denotes mathematical expectation.

Using shared communications knowledge, it is assumed that the radar receiver can decode and reconstruct the communications signal accurately enough [16], [19]. Thus, it is easy to see that $r_n[k] \sim \mathcal{CN}(\mu_{R,n}[k] + \mu_{C,n}[k], \sigma_w^2)$, where

$$\begin{aligned}\mu_{R,n}[k] &= \sum_{m=1}^{M_R} \sqrt{E_{R,m}}\zeta_{R,nm}s_{R,m}(kT_s - \tau_{R,nm})e^{j2\pi f_{R,nm}kT_s},\\ \mu_{C,n}[k] &= \sum_{m'=1}^{M_C} \sqrt{E_{C,m'}}\zeta_{C,nm'}s_{C,m'}(kT_s - \tau_{C,nm'})e^{j2\pi f_{C,nm'}kT_s},\end{aligned} \tag{2}$$

and the symbol $\mathcal{CN}(\mu, \sigma^2)$ implies complex Gaussian distribution with mean μ and variance σ^2.

Thus, the real and imaginary parts of $r_n[k]$ are independent and Gaussian distributed,

$$\begin{aligned}Re\{r_n[k]\} &\sim \mathcal{N}(\mu_{R,n}^{Re}[k] + \mu_{C,n}^{Re}[k], \sigma_n^2),\\ Im\{r_n[k]\} &\sim \mathcal{N}(\mu_{R,n}^{Im}[k] + \mu_{C,n}^{Im}[k], \sigma_n^2),\end{aligned} \tag{3}$$

where $\sigma_n^2 = \sigma_w^2/2$, $\mu_{R,n}^{Re}[k] = Re\{\mu_{R,n}[k]\}$, $\mu_{R,n}^{Im}[k] = Im\{\mu_{R,n}[k]\}$, $\mu_{C,n}^{Re}[k] = Re\{\mu_{C,n}[k]\}$, $\mu_{C,n}^{Im}[k] = Im\{\mu_{C,n}[k]\}$, the $\mathcal{N}(\mu, \sigma^2)$ implies a real Gaussian distribution with mean μ and variance σ^2, and $Re\{\cdot\}$ and $Im\{\cdot\}$ denote taking the real part and imaginary part.

Collecting all time samples, the signal vector received at receiver n can be written as

$$\mathbf{r}_n = [r_n[1], \cdots, r_n[K]]^\dagger = \boldsymbol{\mu}_{R,n} + \boldsymbol{\mu}_{C,n} + \mathbf{w}_n, \tag{4}$$

wher the superscript "†" denotes transpose, $\boldsymbol{\mu}_{R,n} = [\mu_{R,n}[1], \cdots, \mu_{R,n}[K]]^\dagger$, $\boldsymbol{\mu}_{C,n} = [\mu_{C,n}[1], \cdots, \mu_{C,n}[K]]^\dagger$, and $\mathbf{w}_n = [w_n[1], \cdots, w_n[K]]^\dagger$.

III. Quantization-Based Detection

In the cooperative IRC system, to cope with the hardware complexity, the low resolution ADC is used. The received signals are quantized at each radar receiver and then transmitted to the FC. Consider a D-level quantizer $\mathbb{Q}$ with a possible quantization value set $\boldsymbol{V}$ and quantizer thresholds $\boldsymbol{\gamma}$, where

$$\boldsymbol{V} = [V_0, V_1, \cdots, V_{D-1}]^\dagger \tag{5}$$

and $-\infty = \gamma_0 < \gamma_1 < \cdots < \gamma_D = +\infty$. The output of the quantizer $\mathbb{Q}$ to input x is denoted by

$$\mathbb{Q}\{x\} = V_d \quad \text{when} \quad x \in (\gamma_d, \gamma_{d+1}] \tag{6}$$

for $d = 0, \cdots, D-1$.

For the complex received signal $r_n[k]$, we employ two quantizers of the same design separately to quantize the real and imaginary parts, where the quantizer is described as (6). When using a uniform quantizer with a dynamic range $[-\gamma, \gamma]$, the quantization thresholds are $\gamma_0 = -\infty$, $\gamma_D = \infty$, $\gamma_d = [d - (D-1)/2 - 1]\Delta_{\text{co}}$, for $d = 1, \cdots, D-1$, where $\Delta_{\text{co}} = 2\gamma/2^b$, and b is the number of quantization bits.

At each local sensor, the output of the quantizer $q_n[k]$ can be expressed as

$$q_n[k] = \mathbb{Q}\{Re\{r_n[k]\}\} + j\mathbb{Q}\{Im\{r_n[k]\}\}. \tag{7}$$

For hypothesis H_0, it can be obtained that for $d_{R,nk} \in \{0, 1, \cdots, D-1\}, d_{I,nk} \in \{0, 1, \cdots, D-1\}$

$$\begin{aligned}P(q_n[k]|H_0) &= P(Re\{q_n[k]\} = V_{d_{R,nk}}, Im\{q_n[k]\} = V_{d_{I,nk}}|H_0)\\ &= \left[Q\left(\gamma_{d_{R,nk}}/\sigma_n\right) - Q\left(\gamma_{d_{R,nk}+1}/\sigma_n\right)\right]\\ &\quad \times \left[Q\left(\gamma_{d_{I,nk}}/\sigma_n\right) - Q\left(\gamma_{d_{I,nk}+1}/\sigma_n\right)\right],\end{aligned} \tag{8}$$

where $Q(x)$ is the complementary distribution function of the Gaussian distribution defined as

$$Q(x) = \int_x^\infty \frac{1}{\sqrt{2\pi}} e^{-\frac{x^2}{2}} dt. \tag{9}$$

Similarly, for hypothesis H_1 we have

$$\begin{aligned}P(q_n[k]|H_1) &= \left[Q\left((\gamma_{d_{R,nk}} - \mu_{R,n}^{Re}[k] - \mu_{C,n}^{Re}[k])/\sigma_n\right)\right.\\ &\quad \left. - Q\left((\gamma_{d_{R,nk}+1} - \mu_{R,n}^{Re}[k] - \mu_{C,n}^{Re}[k])/\sigma_n\right)\right]\\ &\quad \times \left[Q\left((\gamma_{d_{I,nk}} - \mu_{R,n}^{Im}[k] - \mu_{C,n}^{Im}[k])/\sigma_n\right)\right.\\ &\quad \left. - Q\left((\gamma_{d_{I,nk}+1} - \mu_{R,n}^{Im}[k] - \mu_{C,n}^{Im}[k])/\sigma_n\right)\right].\end{aligned} \tag{10}$$

To simplify analysis, assume that the data transmission between the local sensor and the FC is ideal. At the FC, the observation vector received is

$$\mathbf{y} = \mathbf{q}, \tag{11}$$

where $\mathbf{q} = \left(\mathbf{q}_1^\dagger \cdots \mathbf{q}_N^\dagger\right)^\dagger$, in which $\mathbf{q}_n = [q_n[1] \cdots q_n[K]]^\dagger$. Therefore, under the two different hypotheses, the detection problem at the FC is

$$\begin{aligned}H_0 &: \mathbf{y} = \mathbf{q} = (q_1[1]|H_0,\ q_1[2]|H_0,\ \cdots\ q_N[K]|H_0)^\dagger,\\ H_1 &: \mathbf{y} = \mathbf{q} = (q_1[1]|H_1,\ q_1[2]|H_1,\ \cdots\ q_N[K]|H_1)^\dagger,\end{aligned} \tag{12}$$

where

$$q_n[k]|H_0 = \mathbb{Q}\{Re\{w_n[k]\}\} + j\mathbb{Q}\{Im\{w_n[k]\}\} \tag{13}$$

and

$$\begin{aligned}q_n[k]|H_1 &= \mathbb{Q}\left\{Re\left\{\mu_{R,n}^*[k] + \mu_{C,n}^*[k] + w_n[k]\right\}\right\}\\ &\quad + j\mathbb{Q}\left\{Im\left\{\mu_{R,n}^*[k] + \mu_{C,n}^*[k] + w_n[k]\right\}\right\}.\end{aligned} \tag{14}$$

The likelihood functions are thereby $P(\mathbf{y}|H_0) = \prod_{n=1}^{N}\prod_{k=1}^{K} P(q_n[k]|H_0)$ and $P(\mathbf{y}|H_1) = \prod_{n=1}^{N}\prod_{k=1}^{K} p(q_n[k]|H_1)$. Accordingly, the log-likelihood ratio can be computed as

$$L_{\text{co}} = \ln\frac{p(\mathbf{y}|H_1)}{p(\mathbf{y}|H_0)} = \sum_{n=1}^{N}\sum_{k=1}^{K} \ln\frac{p(q_n[k]|H_1)}{p(q_n[k]|H_0)}. \tag{15}$$

Substituting (8) and (10) into (15), the log-likelihood ratio can be obtained. Applying the Neyman-Pearson criterion, the detection probability for the cooperative IRC system is

$$P_{\text{D,co}} = Pr(L_{\text{co}} \geq \alpha|H_1), \tag{16}$$

where α is the detection threshold determined by the false

alarm level $P_{\text{FA,co}} = Pr\left(L_{\text{co}} > \alpha | H_0\right)$.

According to [20, *Theorem 1*], when the uniform quantization interval Δ is small enough compared with the variance of the input noise σ^2, the quantization output can be approximated to a Gaussian distribution with mean μ and variance $\sigma^2 + \Delta^2/12$, where μ and σ^2 are the mean and variance of the Gaussian quantization input, respectively. Hence, when the quantization interval is small enough, the distribution of $q_n[k]$ is

$$q_n[k]\,|H_0 \sim \mathcal{N}\left(0, \sigma_w^2 + \Delta_{\text{co}}^2/6\right), \tag{17}$$

$$q_n[k]\,|H_1 \sim \mathcal{N}\left(\mu_{R,n}[k] + \mu_{C,n}[k], \sigma_w^2 + \Delta_{\text{co}}^2/6\right). \tag{18}$$

From (17) and (18), the log-likelihood ratio in (15) can be calculated, and then the test statistic is given by

$$T_{\text{co}} = \sum_{n=1}^{N}\sum_{k=1}^{K} Re\{q_n^*[k](\mu_{R,n}[k] + \mu_{C,n}[k])\}, \tag{19}$$

where

$$T_{\text{co}}|H_0 \sim \mathcal{N}\left(0, \sigma_{\text{co}}^2\right),\ T_{\text{co}}|H_1 \sim \mathcal{N}\left(\mu_{\text{co}}, \sigma_{\text{co}}^2\right), \tag{20}$$

in which

$$\sigma_{\text{co}}^2 = \sum_{n=1}^{N}\sum_{k=1}^{K} \left|\mu_{R,n}[k] + \mu_{C,n}[k]\right|^2 \left(\sigma_w^2 + \Delta_{\text{co}}^2/6\right)/2, \tag{21}$$

and

$$\mu_{\text{co}} = \sum_{n=1}^{N}\sum_{k=1}^{K} \left|\mu_{R,n}[k] + \mu_{C,n}[k]\right|^2. \tag{22}$$

Thus, for a sufficiently small quantization interval, the detection probability can be calculated as

$$P_{\text{D,co}} = Q\left(Q^{-1}\left(P_{\text{FA,co}}\right) - \frac{\mu_{\text{co}}}{\sigma_{\text{co}}}\right), \tag{23}$$

where σ_{co} and μ_{co} are defined in (22) and (21), respectively.

IV. Cooperation Gains

In the cooperative system, target returns contributed from both the radar transmitters and communications transmitters are employed to complete the radar task, forming an hybrid active-passive MIMO radar. In this section, in order to demonstrate the performance advantages for the cooperative system, the detection performance of the cooperative case is compared with the non-cooperative case where only the radar signals are considered without the influence of the communications signals.

The signal vector received at receiver n for the non-cooperative case can be written as

$$\mathbf{r}_n = \boldsymbol{\mu}_{R,n} + \mathbf{w}_n. \tag{24}$$

Using analysis similar to the cooperative system, the detection probability for the non-cooperative case can be obtained, which is

$$P_{\text{D,non}} = Q\left(Q^{-1}\left(P_{\text{FA,non}}\right) - \frac{\mu_{\text{non}}}{\sigma_{\text{non}}}\right), \tag{25}$$

where $\sigma_{\text{non}}^2 = \sum_{n=1}^{N}\sum_{k=1}^{K} \left|\mu_{R,n}[k]\right|^2 \left(\sigma_w^2 + \Delta_{\text{non}}^2/6\right)/2$, $\mu_{\text{non}} = \sum_{n=1}^{N}\sum_{k=1}^{K} \left|\mu_{R,n}[k]\right|^2$, $P_{\text{FA,non}}$ is the corresponding false alarm probability, and Δ_{non} is the corresponding quantization interval.

Next, we compare the performance of the cooperative and non-cooperative cases as stated in the following theorem. To simplify analysis, assume the radar and communications signals are approximately orthogonal. Define the radar signal to clutter-plus-noise ratio and communications signal to clutter-plus-noise ratio as

$$\text{SCNR}_R = \sum_{n=1}^{N}\sum_{k=1}^{K} |\mu_{R,n}[k]|^2/N\sigma_w^2, \tag{26}$$

$$\text{SCNR}_C = \sum_{n=1}^{N}\sum_{k=1}^{K} |\mu_{C,n}[k]|^2/N\sigma_w^2. \tag{27}$$

Theorem 1. When the quantization interval is small enough, there is a radar detection performance gain due to the cooperation between the radar and communications systems under the same parameter settings, i.e.

$$P_{\text{D,co}} \geq P_{\text{D,non}}, \tag{28}$$

and when the communications signal to clutter-plus-noise ratio SCNR_C equals zero, the equality holds. With the increase of SCNR_C, the detection performance gain from cooperation becomes larger.

Proof: From (23) and (25), it can be seen that the performance for the cooperative and non-cooperative cases depends on $\frac{\mu_{\text{co}}}{\sigma_{\text{co}}}$ and $\frac{\mu_{\text{non}}}{\sigma_{\text{non}}}$, respectively, where

$$\frac{\mu_{\text{co}}}{\sigma_{\text{co}}}\Big/\frac{\mu_{\text{non}}}{\sigma_{\text{non}}} = \frac{\sum_{n=1}^{N}\sum_{k=1}^{K} \left|\mu_{R,n}[k] + \mu_{C,n}[k]\right|^2}{\sum_{n=1}^{N}\sum_{k=1}^{K} \left|\mu_{R,n}[k]\right|^2} \times \sqrt{\frac{\sum_{n=1}^{N}\sum_{k=1}^{K} \left|\mu_{R,n}[k]\right|^2(\sigma_w^2 + \Delta_{\text{non}}^2/6)}{\sum_{n=1}^{N}\sum_{k=1}^{K} \left|\mu_{R,n}[k] + \mu_{C,n}[k]\right|^2(\sigma_w^2 + \Delta_{\text{co}}^2/6)}}. \tag{29}$$

According to the definition SCNR_R in (26) and SCNR_C in (27), we have

$$\frac{\mu_{\text{co}}}{\sigma_{\text{co}}}\Big/\frac{\mu_{\text{non}}}{\sigma_{\text{non}}} = \sqrt{\frac{(\text{SCNR}_{\text{R}} + \text{SCNR}_{\text{C}})(\sigma_w^2 + \Delta_{\text{non}}^2/6)}{\text{SCNR}_{\text{R}}(\sigma_w^2 + \Delta_{\text{co}}^2/6)}}. \tag{30}$$

Under the same quantization interval, i.e. $\Delta_{\text{co}} = \Delta_{\text{non}}$, from (30), we have

$$\frac{\mu_{\text{co}}}{\sigma_{\text{co}}}\Big/\frac{\mu_{\text{non}}}{\sigma_{\text{non}}} \geq 1, \tag{31}$$

which indicates the detection probability for cooperative case is bigger than that for the non-cooperative case, i.e. $P_{\text{D,co}} \geq P_{\text{D,non}}$. Thus, there is a radar detection performance gain through cooperation.

Futher, from (30), we know that with the increase of SCNR_C, $\frac{\mu_{\text{co}}}{\sigma_{\text{co}}}/\frac{\mu_{\text{non}}}{\sigma_{\text{non}}}$ becomes larger. Based on (23) and (25), with the increase of $\frac{\mu_{\text{co}}}{\sigma_{\text{co}}}/\frac{\mu_{\text{non}}}{\sigma_{\text{non}}}$, the performance gain from cooperation is bigger. When $\text{SCNR}_C = 0$, it can be obtained that

$$\frac{\mu_{\text{co}}}{\sigma_{\text{co}}}/\frac{\mu_{\text{non}}}{\sigma_{\text{non}}} = \sqrt{\frac{(\text{SCNR}_{\text{R}} + 0)(\sigma_w^2 + \Delta_{non}^2/6)}{\text{SCNR}_R(\sigma_w^2 + \Delta_{co}^2/6)}} = 1, \quad (32)$$

that is, $\frac{\mu_{\text{co}}}{\sigma_{\text{co}}} = \frac{\mu_{\text{non}}}{\sigma_{\text{non}}}$. From (23) and (25), when $\frac{\mu_{\text{co}}}{\sigma_{\text{co}}} = \frac{\mu_{\text{non}}}{\sigma_{\text{non}}}$, $P_{\text{D,co}} = P_{\text{D,non}}$, which indicetes that when $\text{SCNR}_C = 0$ the equality in (28) holds.

□

V. Numerical Examples

In this section, we use examples to illustrate the performance of the cooperative IRC system. Assume the system has $M_R = 4$ radar transmitters, $M_C = 5$ communications transmitters, and $N = 20$ radar receivers. All radar and communications stations are located 6 km away from the origin of the coordinate system. Suppose the cell under test is centered at $(0, 0)m$ moving with velocity $(25, 20)km/h$. The radar transmitted signals are frequency spread single Gaussian pulse signals, given by

$$s_m(kT_s) = (\frac{2}{T^2})^{1/4} e^{(-\pi(kT_s)^2/T^2)} e^{j2\pi m f_\Delta kT_s}, \quad (33)$$

where f_Δ is the frequency offset between adjacent radar transmit signals and T the pulsewidth. Set $f_\Delta = 500Hz$, $f_s = 2000Hz$ and $T = 0.01s$. The communications transmitted signals are the orthogonal frequency division multiplexing signals

$$s_{m'}(t) = \sum_{n=-N_f/2}^{N_f/2-1} a_{m'}[n] e^{j2\pi n \Delta f t}, \quad (34)$$

where T' is the pulsewidth, Δf is the frequency spacing between two adjacent subcarriers, N_f is the number of subcarriers, and $a_{m'}[n]$ are data symbols. Let $T' = 0.01s$, $\Delta f = 125$ Hz, and $N_f = 6$. The signal to clutter-plus-noise is defined as $\text{SCNR} = \text{SCNR}_R + \text{SCNR}_C$. Set $\sigma_w^2 = 1$ and $\text{SCNR} = -6.5dB$. The dynamic range of the quantizer is $\gamma = 6$.

A. Detection Performance

In Fig. 1, the detection probability P_D versus the false alarm probability P_{FA} is plotted under different number of quantization bits b. The analytical results (Theo) obtained from (23) and the simulated results (Sim) are represented by the solid and dash curves, respectively. For comparison, the unquantized results, which can be obtained from (23) by setting $\Delta_{\text{co}} = 0$, are also shown. From the figure, the simulated results are close to the analytical results for a suitably large

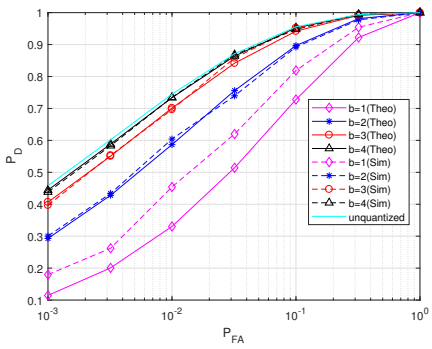

Fig. 1: Detection probability under different number of quantization bits b.

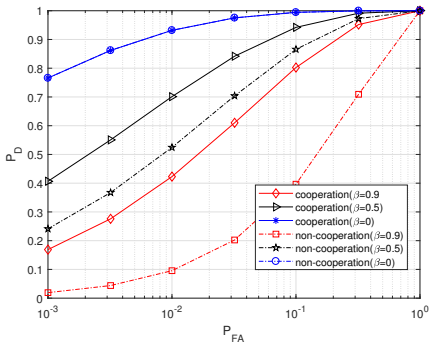

Fig. 2: Detection probability under different β for the cooperative and non-cooperative systems with $b = 3$.

number of quantization bits, such as $b \geq 2$ in our example, which supports the correctness of the derived expression for P_D in (23). For a sufficiently small number of quantization bits, e.g. $b = 1$ in this example, the quantization interval is large compared with the variance of the quantization input, so the quantization output cannot be approximated to obey a Gaussian distribution [20], resulting in the analytical and simulated results being different.

B. Cooperative and Non-cooperative Cases

Denote the ratio of SCNR_C and SCNR as β, that is, $\text{SCNR}_C = \beta\text{SCNR}$. Fig. 2 illustrates the detection probabilities P_D versus the false alarm probability P_{FA} under a different β for cooperative and non-cooperative cases when $b = 3$. The resulting curves show that, the detection probabilities for the cooperative system are always greater than those for the non-cooperative case, indicating that there is a radar detection performance gain due to the cooperation between the radar and communications systems, as predicted by *Theorem 1*. With the increase of β, the radar signal to clutter-plus-noise ratio SCNR_R decreases, so the corresponding detection performance decreases for both the cooperative and non-cooperative system. When $\beta = 0$, $\text{SCNR}_C = 0$, and the detection performance of the cooperative and non-cooperative system is the same, as stated in *Theorem 1*.

VI. Conclusion

In this paper, quantization-based target detection was investigated for a cooperative IRC network with distributed radar and communications system. The detection probability for the likelihood ratio test was derived in closed-form for the cooperative IRC system, which was then compared with the non-cooperative case analytically. We demonstrated that there is a radar detection performance gain due to the cooperation between the radar and communications systems. With the increase of communications signal to clutter-plus-noise ratio SCNR_C, the performance gain from cooperation becomes larger, and the cooperative system has the same performance as the non-cooperative system when SCNR_C equals zero.

References

[1] S. H. Dokhanchi, B. S. Mysore, K. V. Mishra, and B. Ottersten, "A mmwave automotive joint radar-communications system," *IEEE Transactions on Aerospace and Electronic Systems*, vol. 55, no. 3, pp. 1241–1260, 2019.

[2] D. Ma, N. Shlezinger, T. Huang, Y. Liu, and Y. C. Eldar, "Joint radar-communication strategies for autonomous vehicles: Combining two key automotive technologies," *IEEE Signal Processing Magazine*, vol. 37, no. 4, pp. 85–97, 2020.

[3] M. Z. Chowdhury, M. Shahjalal, S. Ahmed, and Y. M. Jang, "6G wireless communication systems: Applications, requirements, technologies, challenges, and research directions," *IEEE Open Journal of the Communications Society*, vol. 1, pp. 957–975, 2020.

[4] D. K. Pin Tan, J. He, Y. Li, A. Bayesteh, Y. Chen, P. Zhu, and W. Tong, "Integrated sensing and communication in 6G: Motivations, use cases, requirements, challenges and future directions," in *2021 1st IEEE International Online Symposium on Joint Communications Sensing (JCS)*, 2021, pp. 1–6.

[5] A. R. Chiriyath, B. Paul, and D. W. Bliss, "Radar-communications convergence: Coexistence, cooperation, and co-design," *IEEE Transactions on Cognitive Communications and Networking*, vol. 3, no. 1, pp. 1–12, March 2017.

[6] L. Zheng, M. Lops, Y. C. Eldar, and X. Wang, "Radar and communication coexistence: An overview: A review of recent methods," *IEEE Signal Processing Magazine*, vol. 36, no. 5, pp. 85–99, 2019.

[7] F. Liu, C. Masouros, A. P. Petropulu, H. Griffiths, and L. Hanzo, "Joint radar and communication design: Applications, state-of-the-art, and the road ahead," *IEEE Transactions on Communications*, vol. 68, no. 6, pp. 3834–3862, 2020.

[8] J. A. Zhang, F. Liu, C. Masouros, R. W. Heath, Z. Feng, L. Zheng, and A. Petropulu, "An overview of signal processing techniques for joint communication and radar sensing," *IEEE Journal of Selected Topics in Signal Processing*, pp. 1–1, 2021.

[9] S. Khalili, O. Simeone, and A. M. Haimovich, "Cloud radio-multistatic radar: Joint optimization of code vector and backhaul quantization," *IEEE Signal Processing Letters*, vol. 22, no. 4, pp. 494–498, April 2015.

[10] P. Kumari, K. U. Mazher, A. Mezghani, and R. W. Heath, "Low resolution sampling for joint millimeter-wave MIMO communication-radar," in *2018 IEEE Statistical Signal Processing Workshop (SSP)*, 2018, pp. 193–197.

[11] S. Zhu, F. Xi, S. Chen, and A. Nehorai, "A low-complexity MIMO dual function radar communication system via one-bit sampling," in *2021 IEEE International Conference on Acoustics, Speech and Signal Processing (ICASSP)*, 2021, pp. 8223–8227.

[12] Z. Cheng, S. Shi, Z. He, and B. Liao, "Transmit sequence design for dual-function radar-communication system with one-bit DACs," *IEEE Transactions on Wireless Communications*, pp. 1–1, 2021.

[13] D.-P. Xia, Y. Zhang, P. Cai, and L. Huang, "An energy-efficient signal detection scheme for a radar-communication system based on the generalized approximate message-passing algorithm and low-precision quantization," *IEEE Access*, vol. 7, pp. 29 065–29 075, 2019.

[14] O. Dizdar, A. Kaushik, B. Clerckx, and C. Masouros, "Rate-splitting multiple access for joint radar-communications with low-resolution DACs," in *2021 IEEE International Conference on Communications Workshops (ICC Workshops)*, 2021, pp. 1–6.

[15] D. Ma, N. Shlezinger, T. Huang, Y. Liu, and Y. C. Eldar, "Bit constrained communication receivers in joint radar communications systems," in *2021 IEEE International Conference on Acoustics, Speech and Signal Processing (ICASSP)*, 2021, pp. 8243–8247.

[16] Q. He, Z. Wang, J. Hu, and R. S. Blum, "Performance gains from cooperative MIMO radar and MIMO communication systems," *IEEE Signal Processing Letters*, vol. 26, no. 1, pp. 194–198, 2019.

[17] Z. Zhang, Z. Du, and W. Yu, "Information theoretic waveform design for OFDM radar-communication coexistence in Gaussian mixture interference," *IET Radar, Sonar and Navigation*, vol. 13, no. 11, pp. 2063–2070, 2019.

[18] M. Bica and V. Koivunen, "Radar waveform optimization for target parameter estimation in cooperative radar-communications systems," *IEEE Transactions on Aerospace and Electronic Systems*, vol. 55, no. 5, pp. 2314–2326, 2019.

[19] C. D. Richmond, P. Basu, R. E. Learned, J. Vian, A. Worthen, and M. Lockard, "Performance bounds on cooperative radar and communication systems operation," in *Proceedings of the 2016 IEEE Radar Conference (RadarConf)*, May 2016, pp. 1–6.

[20] Z. Wang, Q. He, and R. S. Blum, "Target detection using quantized cloud MIMO radar measurements," *IEEE Transactions on Signal Processing*, vol. 70, pp. 1–16, 2022.